

# ISOTHERMAL AND NON-ISOTHERMAL CRYSTALLIZATION KINETICS OF BRANCHED AND PARTIALLY CROSSLINKED PET DSC study

G. Z. Papageorgiou, D. S. Achilias\*, D. N. Bikiaris and G. P. Karayannidis

Laboratory of Organic Chemical Technology, Department of Chemistry, Aristotle University of Thessaloniki, 541 24 Thessaloniki, Macedonia, Greece

The crystallization kinetics of branched and partially crosslinked poly(ethylene terephthalate) (PET), prepared using trimethyl trimellitate as branching agent was studied using DSC and WAXD. Crystallization rates were retarded with increasing branching agent content. Avrami equation was used in the isothermal crystallization, while for the non-isothermal process the Ozawa model was applied. Isothermal crystallization half-times increased with branching agent content and crystallization peak temperatures during cooling, decreased. WAXD showed big broadening and reduced degree of crystallinity compared to the neat polyester. Though, the crystal lattice parameters did not seem to alter, crystal size reduction was evidenced.

**Keywords:** crystallization kinetics, DSC, poly(ethylene terephthalate), trimethyl trimellitate

## Introduction

Thermoplastic polyesters, like poly(ethylene terephthalate) (PET), have adequate mechanical and thermal properties but low melt viscosities and melt strength. Thus, they are unsuitable for the manufacturing of extruded shapes, tubes or blow-moulded products. Moreover, the physical properties of these semicrystalline polymers are strongly affected by their microstructure. Consequently, chemical modification of (PET) by introduction of branching agents is a promising technique to improve its properties and extend its uses in many applications. In general, branched or cross-linked polymers exhibit different rheological characteristics, crystalline behaviour and processing properties compared to the linear ones with the same chemical composition. Multifunctional monomers such as di-, tri-, and tetra-epoxides as well as dianhydrides, multifunctional acids or polyols can act as chain extenders, increasing the molecular mass of the polyester and resulting in branched or crosslinked macromolecules [1–5]. The portion of the branching additive could be very small [6]. In practice, the addition of multifunctional compounds has been introduced in almost all the applications of PET, including films, fibres, bottles, foams, etc. [3, 5].

Crystallization during processing of a polymer determines the morphology and the properties of the final product. Crystallization and melting of PET has been extensively studied in literature [6–10]. The crystallization rate of PET is affected by many fac-

tors, among them molecular mass residual catalysts, comonomers and various additives have been recognized as the most important [11–14]. It is known that random branching alters the crystallization behaviour of linear polymers. However, only a limited number of works described the crystallization of branched PET [6]. In general the crystallization rates are reduced with increasing branching, though for very low branch content the crystallization is nucleated by branches and thus accelerated.

Recently, our group has extensively studied the crystallization kinetics of several polymers [15–16]. In this work, a series of branched and partially cross-linked PET samples were prepared using trimethyl trimellitate (TMT) as polyfunctional monomer and the crystallization behaviour under both isothermal and dynamic conditions was studied using DSC.

## Experimental

Synthesis of linear and branched PET was described in a previous paper [17]. For the synthesis of branched PET several amounts of TMT were used instead of dimethyl terephthalate (DMT) such as 0.25, 0.5, 0.875, 1.25 mass% based on DMT. Intrinsic viscosities of the polyesters were measured with an Ubbelohde viscometer at 25°C in mixture of phenol and tetrachloroethane (60/40 mass/mass). Calorimetric measurements were performed on a PerkinElmer Pyris 1 DSC. Dynamic crystallization experiments

\* Author for correspondence: axilias@chem.auth.gr

were carried out using the DSC and by applying various cooling rates, including 1, 2.5, 5, 10 and 20°C min<sup>-1</sup>. Prior to cooling the samples were melted at 300°C for 5 min to erase any thermal history. For isothermal crystallization kinetic studies, all samples were first heated up to 300°C also for 5 min and then quenched to the predetermined crystallization temperature (in the range 210–225°C) at a cooling rate 250°C min<sup>-1</sup>. To prevent degradation of the polyesters a fresh sample was used in each test and all tests were performed under a nitrogen atmosphere (flow rate 20 mL min<sup>-1</sup>). WAXD study was performed over the range 2θ from 5 to 55°, at steps of 0.05° and counting time 5 s, using a Philips PW1710 powder diffractometer, with CuK<sub>α</sub> Nickel-filtered radiation.

The values of the intrinsic viscosity, number average molecular mass and branching coefficient for the polyesters studied are included in Table 1. Branching coefficient or number average branching density expresses the average number of branches per molecule. Since this value was very high for 0.875 mass% TMT content it could not be determined.

**Table 1** Intrinsic viscosity, number average molecular mass and branching coefficient of the linear and branched PET polyesters [17]

TMT/mass%	$\eta/\text{dL g}^{-1}$	$\bar{M}_n/\text{g mol}^{-1}$	$\bar{B}_n$
0	0.79	23000	0
0.250	0.86	26000	0.296
0.500	1.03	37500	1.206
0.875	1.53	63300	–

## Results and discussion

In the WAXD patterns of the as received branched PET samples, shown in Fig. 1, the same crystal reflections as for the neat PET resin appeared. Though the crystal lattice parameters did not seem to alter, since no changes in peak positions were observed, crystal size reduction was evidenced by some change in the ratio of peak height/width. Also, crystallinity was reduced with increasing TMT content. Since all the samples were left to crystallize from the melt by cooling the reactor in air, differences should be attributed to the composition of the samples alone.

Crystallization rates of the resins were studied under both isothermal and non-isothermal conditions. In the isothermal experiments, a series of crystallizations were carried out for each sample at temperatures in the range 210–225°C. The time corresponding to the maximum of the peak was determined directly from the crystallization exotherms and plots of time to peak *vs.* crystallization temperature were constructed (Fig. 2). It was observed that the introduction of branches in PET, increased the rate of crystallization

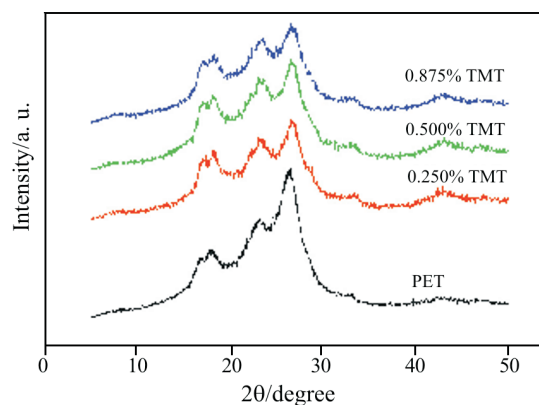


**Fig. 1** WAXD patterns of branched PET samples

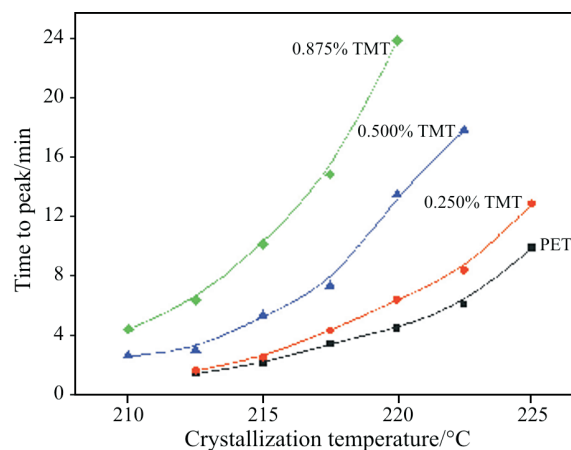


**Fig. 2** Time corresponding to the maximum of the peak ( $t_p$ ), as a function of isothermal crystallization temperature for the linear and branched PET samples

(inverse of the crystallization time) markedly and the 0.875% TMT content exhibited the highest crystallization rate at all temperatures. However, for low TMT content, crystallization rates were not significantly affected. It was also observed that the induction times were not increased substantially for branched PET, though overall crystallization rates were reduced. This was because branching of PET favors nucleation, or the increased melt viscosity of the branched samples does not promote complete destruction of the crystal nuclei on melting.

For the analysis of the isothermal crystallization kinetics, the Avrami (Johnson-Mehl-Avrami) equation has been applied [18, 19]. Relative crystallinity,  $X(t)$ , is related to the crystallization time,  $t$ , according to:

$$X(t) = 1 - \exp(-kt^n) \quad \text{or} \quad X(t) = 1 - \exp[-(Kt)^n] \quad (1)$$

where,  $n$  is the Avrami exponent which is a function of the nucleation process and  $k$  is the growth function, which is dependent on nucleation and crystal growth. Since the units of  $k$  are a function of  $n$ , Eq. (1) can be written in the composite – Avrami form using  $K$  instead of  $k$  (where  $k=K^n$ ) [20]. The values of  $n$ ,  $k$  and  $K$ ,

**Table 2** Half-time of crystallization, Avrami parameters  $n$  and  $k$ ,  $T_g$ ,  $T_m^0$  and nucleation parameter,  $K_g$  from the Lauritzen-Hoffman analysis for isothermal crystallization of linear and branched PET samples

Samples	$T/^\circ\text{C}$	$t_{1/2}-t_0/\text{min}$	$n$	$k/\text{min}^{-n}$	$T_g/^\circ\text{C}$	$T_m/^\circ\text{C}$	$T_m^0/^\circ\text{C}$	$K_g/\text{K}^2$
PET	215.0	2.41	2.5	0.084	81	254	280	$3.7 \cdot 10^5$
	217.5	3.85	2.5	0.026				
	220.0	4.52	2.4	0.020				
	222.5	6.73	2.4	0.007				
	225.0	12.5	2.4	0.002				
TMT-0.25%	215.0	2.97	2.1	0.081	82.5	250	279	$4.2 \cdot 10^5$
	217.5	6.72	2.0	0.018				
	220.0	7.24	2.3	0.010				
TMT-0.50%	222.5	10.9	2.0	0.007	83	249	276	$4.8 \cdot 10^5$
	210.0	4.21	1.5	0.087				
	212.5	7.04	2.0	0.010				
	215.0	8.89	2.0	0.009				
TMT-0.875%	217.5	15.2	2.0	0.003	83	246	279	$5.1 \cdot 10^5$
	207.5	6.00	2.0	0.022				
	210.0	8.55	2.0	0.011				
	212.5	15.5	2.0	0.004				
	215.0	18.2	2.0	0.002				

can be calculated from fitting to experimental data using the double logarithmic form of Eq. (1):

$$\ln\{-\ln[1-X(t)]\} = \ln k + n \ln t \quad (2)$$

From the plots of the left-hand side of Eq. (2) vs.  $\ln(t)$  straight lines were observed for every temperature, which allowed the estimation of the parameters  $n$  and  $k$  from the slope and the intercept, respectively. These values are summarized in Table 2. Notice here that in the fitting only the relative crystallinity data in the range 10–80% were used.

The  $n$  values found in the case of PET were in the vicinity of 2.5. This probably corresponds to a three-dimensional growth with a combination of thermal and athermal nucleation (resulting in the fractional values of  $n$  observed). These values are in good agreement with corresponding literature data, reported by Lu and Hay ( $n=2.6$ ) [21]. From the data of Table 2 it can be observed that for branched samples the values of  $n$  are smaller than those calculated for linear PET. The decrease of  $n$  with the branching might be explained on the basis of a modification in the crystalline morphology due to a reduced mobility of the polymer chains. Furthermore,  $k$  was very sensitive in changes in the  $T_c$ . As the crystallization temperature increased the growth function significantly decreased as it was also observed for the  $1/t_{1/2}$  values. Furthermore, lower values for  $k$  were observed as the branching content was increased. This is in accordance with the results observed in the  $t_{1/2}$  values.

The kinetic data of isothermal crystallization were also analyzed using the spherulitic growth rate in the context of the Lauritzen-Hoffman secondary nucleation theory [22]. Accordingly, the growth rate  $G$  is given as a function of the crystallization temperature,  $T_c$ , by the following biexponential equation:

$$G = G_0 \exp\left[-\frac{U^*}{R(T_c - T_\infty)}\right] \exp\left[-\frac{K_g}{T_c(\Delta T)f}\right] \quad (3)$$

where,  $G_0$  is the pre-exponential factor, the first exponential term contains the contribution of diffusion process to the growth rate, while the second exponential term is the contribution of the nucleation process;  $U^*$  denotes the activation energy and  $T_\infty$  set equal to  $T_g - 30$  (K);  $K_g$  is a nucleation constant given as a function of the side and fold surface free energies, the single layer thickness and the enthalpy of melting and  $\Delta T$  denotes the degree of undercooling ( $\Delta T = T_m^0 - T_c$ );  $f$  is a correction factor which is close to unity at high temperatures and is given as  $f = 2T_c/(T_m^0 + T_c)$ ; the equilibrium melting temperature,  $T_m^0$  can be calculated using some extrapolative procedure like the linear or non-linear Hoffman-Weeks extrapolation. The nucleation parameter,  $K_g$ , can be calculated from Eq. (3) using the double logarithmic transformation:

$$\ln(G) + \frac{U^*}{R(T_c - T_\infty)} = \ln(G_0) - \frac{K_g}{T_c(\Delta T)f} \quad (4)$$

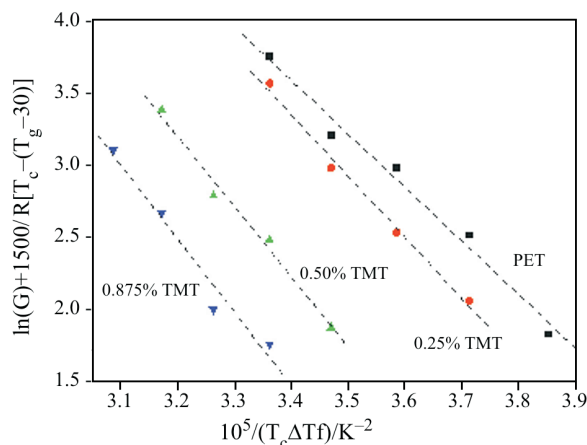


**Fig. 3** Lauritzen-Hoffman type plots of linear and branched PET samples using  $1/t_{1/2}$  in place of  $G$

Plotting the left-hand side of Eq. (4) with respect to  $1/(T_c(\Delta T)f)$  a straight line should appear having a slope equal to  $K_g$ . These plots for linear and branched PET are illustrated in Fig. 3 and a linear behavior is observed in all cases. The  $K_g$  values calculated from the slope of these lines are reported in Table 2. The values obtained were found to increase with the branching content, as it was reported in literature for branched PBT [23]. Thus, the results suggest that the presence of branching hinders the folding of the macromolecular chain.

Furthermore, the melting behavior of the isothermally crystallized samples was studied. Multiple melting was observed in all samples, while this was less obvious for high TMT content. According to the Hoffman-Weeks scheme, the equilibrium melting points of the polyesters were determined by plotting the melting point as a function of the crystallization temperature [24]. It was found that for the TMT-0.875 the  $T_m^0$  was higher than that of the TMT-0.50 (Table 2), in contrast to the melting point that it was found to decrease continuously with the branching content [17]. This was attributed to the fact that since all polyesters were crystallized till complete crystallization, and this polyester had significantly reduced crystallization rates, its crystallization needed much longer times. Prolonged crystallization at high temperatures resulted in significant thickening of the polyester crystals and thus the results were not comparable. This is a serious problem especially for polyesters, since the Hoffman-Weeks process is valid only for a given thickening coefficient.

Furthermore, non-isothermal crystallization kinetics was examined by cooling the samples from the melt. DSC traces of the polyesters recorded at a cooling rate  $10^\circ\text{C min}^{-1}$  are shown in Fig. 4. A displacement of the crystallization peak towards lower temperatures was observed as the TMT content in-

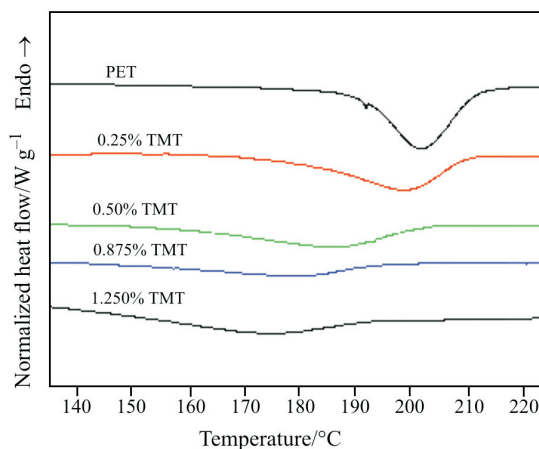


**Fig. 4** DSC traces of linear and branched PET during cooling at  $10^\circ\text{C min}^{-1}$

creased. For the TMT-0.875 and TMT-1.25 a shift of the crystallization temperature by about 25 and  $30^\circ\text{C}$ , respectively was found. Moreover, a significant reduction in the heat of the crystallization peak can be seen, which means a significant decrease of the final crystallinity achieved, together with a peak broadening with increasing TMT content.

For the non-isothermal study various cooling rates from 1 to  $20^\circ\text{C min}^{-1}$  were applied. In Fig. 5, the crystallization peak temperatures are plotted vs. cooling rate. For a given TMT content the peak temperature, as it was anticipated, was shifted to lower values by increasing cooling rate. For a given cooling rate, the peak temperature decreased with increasing TMT content that is the crystallization rate was retarded. The differences in peak temperatures were increased at higher cooling rates. Also, the shapes of the curves were different, since the drop in crystallization temperature is more abrupt at higher TMT content.

In order to quantitatively describe the evolution of crystallinity during non-isothermal crystallization a number of models have been proposed in literature [15, 16]. In this investigation, the Ozawa [25], analy-

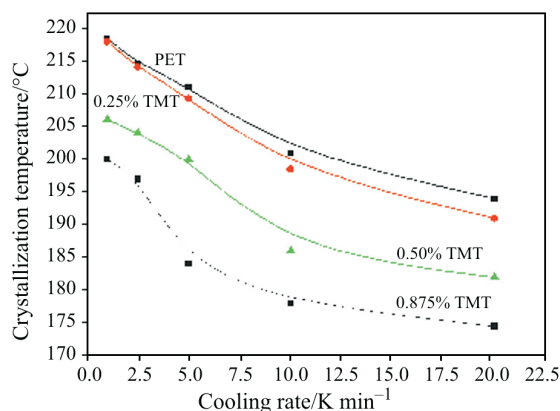


**Fig. 5** Crystallization peak temperature ( $T_c$ ) as a function of the cooling rate

sis was tested. According to this theory, the non-isothermal crystallization process is the result of an infinite number of small isothermal crystallization steps and the degree of conversion at temperature  $T$ ,  $X(T)$ , can be calculated as:

$$\ln[1 - X(T)] = -K^*(T)/\alpha^m \quad (5)$$

where  $m$  is the Ozawa exponent that depends on the dimension of crystal growth and  $K^*$  is the cooling crystallization function.  $K^*$  is related to the overall crystallization rate and indicates how fast crystallization occurs. Taking the double-logarithmic form of Eq. (5), it follows

$$\ln\{-\ln[1 - X(T)]\} = \ln K^*(T) - m \ln \alpha \quad (6)$$

By plotting  $\ln\{-\ln[1 - X(T)]\}$  vs.  $\ln \alpha$ , a straight line should be obtained and the kinetic parameters,  $m$  and  $K^*$ , can be achieved from the slope and the intercept respectively. Ozawa plots for dynamic crystallization of the TMT-0.25 are shown in Fig. 6. In the Ozawa plots of the branched and linear PET samples, increased curvature was observed. The Ozawa exponent  $m$  was always less than the Avrami exponent  $n$  and takes the following values 0.85, 0.85, 1.0, 1.24, 1.77, 2.05 and 2.0 corresponding to temperatures 180, 185, 190, 195, 200, 205 and 210°C, respectively.

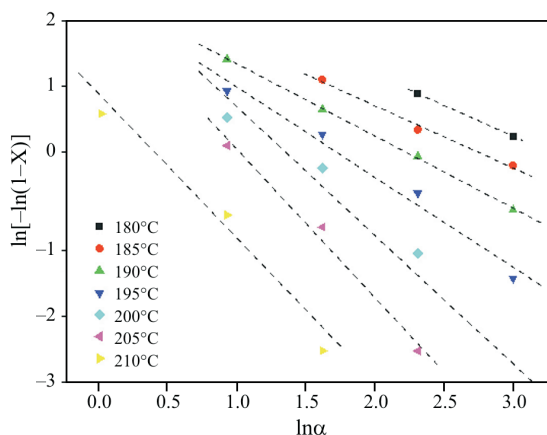


Fig. 6 Ozawa plots for non-isothermal crystallization of the TMT-0.25 sample

## Conclusions

Crystallization rates for branched PET samples were studied under both isothermal and dynamic conditions and were found to reduce with increasing branching agent content. A systematic decrease in crystallization peak temperature was observed for a given cooling rate by increasing branching content. Consequently, not only lower final crystallinity, but also less poor crystals are anticipated to produce for branched PET during dynamic processing. The

Ozawa exponents for non-isothermal crystallization were found to be lower than the Avrami exponents obtained from isothermal data. The  $K_g$  parameter of the Lauritzen-Hoffman was found to increase with branching content representing an increase in the surface free energy.

## References

- 1 M. Xanthos, M. W. Young, G. P. Karayannidis and D. N. Bikiaris, *Polym. Eng. Sci.*, 41 (2001) 643.
- 2 K. H. Yoon, B. G. Min and O. O. Park, *Polym. Int.*, 51 (2002) 134.
- 3 C. Hess, P. Hirt and W. Oppermann, *J. Appl. Polym. Sci.*, 74 (1999) 728.
- 4 S. A. Jabarin, *J. Appl. Polym. Sci.*, 34 (1987) 102.
- 5 R. F. Rosu, R. A. Shanks and S. N. Bhattacharya, *Polymer*, 40 (1999) 5891.
- 6 G. Li, S. L. Yang, J. M. Jiang and C. X. Wu, *Polymer*, 46 (2005) 11142.
- 7 S. Vyazovkin, J. Stone and N. Sbirrazzuoli, *J. Therm. Anal. Cal.*, 80 (2005) 177.
- 8 F. Awaja, F. Daver, E. Kosior and F. Cser, *J. Therm. Anal. Cal.*, 78 (2004) 865.
- 9 S. Montserrat, F. Roman and P. Colomer, *J. Therm. Anal. Cal.*, 72 (2003) 657.
- 10 S. Vyazovkin and N. Sbirrazzuoli, *J. Therm. Anal. Cal.*, 72 (2003) 681.
- 11 B. Gunther and H. G. Zachmann, *Polymer*, 24 (1983) 1008.
- 12 F. Pilati, M. Toselli, M. Messori, C. Manzoni, A. Turturo and E. G. Gattiglia, *Polymer*, 38 (1997) 4469.
- 13 F. J. Medellin-Rodriguez, P. J. Phillips, J. S. Lin and R. Campos, *J. Polym. Sci. Polym. Phys.*, 35 (1997) 1757.
- 14 S. J. Oh and B. C. Kim, *J. Polym. Sci. Polym. Phys.*, 39 (2001) 1027.
- 15 G. Z. Papageorgiou, D. S. Achilias, D. N. Bikiaris and G. P. Karayannidis, *Thermochim. Acta*, 427 (2005) 117.
- 16 D. S. Achilias, G. Z. Papageorgiou and G. P. Karayannidis, *J. Polym. Sci. Polym. Phys.*, 42 (2004) 3775.
- 17 D. N. Bikiaris and G. P. Karayannidis, *Polym. Inter.*, 52 (2003) 1230.
- 18 M. J. Avrami, *J. Chem. Phys.*, 7 (1939) 1103, 8 (1940) 212.
- 19 W. A. Johnson and R. F. Mehl, *Trans. Am. Inst. Mining Metall. Eng.*, 135 (1939) 416.
- 20 N. Dangseeyun, P. Shrimoan, P. Supaphol and M. Nithitanakul, *Thermochim. Acta*, 409 (2004) 63.
- 21 X. F. Lu and J. N. Hay, *Polymer*, 42 (2001) 9423.
- 22 J. D. Hoffman, G. T. Davis and J. I. Lauritzen, *Treatise on Solid State Chemistry*, Hannay NB, Ed, Plenum Press, New York, Vol. 3 Chap. 7, 1976.
- 23 M. C. Righetti and A. Munari, *Macromol. Chem. Phys.*, 198 (1997) 363.
- 24 J. D. Hoffman and J. J. Weeks, *J. Chem. Phys.*, 42 (1965) 4301.
- 25 T. Ozawa, *Polymer*, 12 (1971) 150.

DOI: 10.1007/s10973-005-7366-4